

# GIS Based Integration and Evaluation of Multisource Datasets for Forest Damage Investigations

F.-J. Behr<sup>1</sup>    H. Saurer<sup>2</sup>    H.-P. Bähr<sup>1</sup>

<sup>1</sup> Institut für Photogrammetrie und Fernerkundung (IPF)  
Universität Karlsruhe (TH)  
Englerstr. 7, D-7500 Karlsruhe, FRG  
BEHR@DKAUNIOP.BITNET

<sup>2</sup> Geographisches Institut, Universität Würzburg  
Am Hubland, D-8700 Würzburg, FRG

## COMMISSION IV

### Abstract

In the context of a forest damage research project, CIR photographs have been interpreted based on a regular sample point grid. After rectification, these geocoded datasets (tree species, age, damage class ...) form the basis of a geographic database. Other data layers as DTM, road network, stream courses, settlements, and climatic data have been co-registered.

Applied methods of data combination and evaluation are described. The results are discussed with regard to potential reasons for forest damages.

### Zusammenfassung

Im Rahmen des Projektes „Aufbau eines geographischen Informationssystems zur Ermittlung von Waldschäden und ihrer Veränderung“ wurde im Hochschwarzwald eine Waldschadensintensivinventur durchgeführt. Die erhobenen Daten (Baumart, Alterklasse, Schadstufe etc.) bilden die Grundlage einer geographischen Datenbasis. Angewandte Verfahren zur Verknüpfung mit weiteren Daten (Höhe, Hangneigung und -exposition, Verkehrs- und Gewässernetz) werden dargestellt. Die Ergebnisse werden im Hinblick auf mögliche Ursachen neuartiger Waldschäden diskutiert.

## 1 Introduction

In the context of a forest damage research project „*Development of a geographic information system for investigation and monitoring of forest decline*“ multiple layers of information were integrated in a raster based GIS for digital processing and evaluation.

Forest damage and tree species data of three different scales are available within this project. One dataset is of a grid size of 4 x 4 km containing data of the terrestrial forest damage inventory Baden-Württemberg 1985. Additional data with a grid size of 1 x 1 km respectively 25 x 25 m are deduced from aerial CIR photographs. Data achievement of the latter was based on a regular grid (grid interval 0.5 cm in image scale 1:5000). To enable

combination with other geocoded characteristics, rectification to a common ground coordinate system had to be performed. For rectification of this data three methods were developed and implemented.

In this paper the rectification methods are reviewed. Some results of combination with other GIS layers (settlements, rivers, lakes, roads, site conditions and stand characteristics) are presented.

## 2 Study Areas

During this study, two areas in the Black Forest in S-W Germany have been examined: the *Schluchsee* region and the *Kälbelescheuer* region. The Schluchsee region covers an area of 36 km<sup>2</sup>. Its elevation zone (850 – 1350 meters) is predominated by spruce (*Picea abies*) and beech (*Fagus sylvatica*). In the Kälbelescheuer region (600 – 1200 meters) there is a mixture of spruce, beech, and fir (*Abies alba*) stands.

## 3 Rectification of Forest Damage Data

During forest inventories often systematically distributed sample points were used (KÖLBL/TRACHSLER 1980) or proposed (HILDEBRANDT 1984). For this project data achievement was carried out using a regular grid .

For practical use the sample point grid has been plotted on film which was overlaid to the CIR photographs for interpretation. Damages were classified into four classes corresponding to colour in the CIR photographs. Further nine tree species were distinguished. Tree species and damage class of each sample tree were documented on the interpretation film (cf. Fig. 1). A systematic control of the estimation has been carried out to avoid misclassification and to

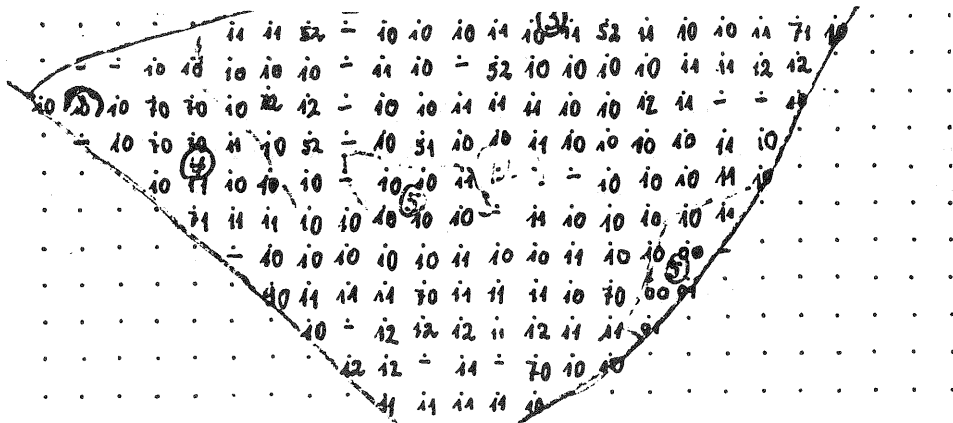


Figure 1: Regular sample tree grid

adjust the results of the different interpreters.

Because no ground control points have been signalled during aerial survey, natural control points, i.e. points which could clearly be recognized in the photographs and in corresponding maps, had to be taken. As far as possible control point coordinates have been digitized from the „Deutsche Grundkarte 1:5000“. For a small part of the inventory area there have not been enough control points in this kind of map. Hence, a portion of control points had to be taken from the topographic map 1:25000 with minor accuracy. A sufficient number of reliable control points (6 – 8 points per photograph) was hard to find.

For geometric rectification, stereo or single image rectification could be used. For stereo rectification, additional restrictions for the control point location exist. Therefore restitution has been performed based on single photographs.

For determination of ground coordinates  $X_i, Y_i, Z_i$  of the sample points three methods were developed and examined:

- projective transformation,
- transformation by image coordinates and terrain height,
- interpolation in an irregular grid.

### 3.1 Projective Transformation

Projective transformation is used to transform between two planes:

$$X_i = \frac{b_{11}x + b_{12}y + b_{13}}{b_{31}x + b_{32}y + 1} \quad Y_i = \frac{b_{21}x + b_{22}y + b_{23}}{b_{31}x + b_{32}y + 1} \quad (1)$$

The eight transformation coefficients  $b_{ij}$  can be determined by at least four identical points in both coordinate systems. Because the transformation lacks a third dimension, there are great horizontal displacements in mountainous regions.

### 3.2 Transformation by image coordinates and terrain height

To avoid horizontal displacements, the terrain height of the sample points and the absolute orientation of the survey camera had to be taken into consideration.

If we do not know the absolute orientation the coordinates  $X_0, Y_0, Z_0$  of the camera position and the rotation angles  $\phi, \omega, \kappa$  can be derived from control points by spatial resection. The connection between ground coordinates  $X_i, Y_i, Z_i$  and corresponding image coordinates  $x_b, y_b$  is given by the collinearity equations (Eq. 2).

$$x_B = -c \frac{a_1(X_i - X_0) + a_2(Y_i - Y_0) + a_3(Z_i - Z_0)}{c_1(X_i - X_0) + c_2(Y_i - Y_0) + c_3(Z_i - Z_0)} \quad (2)$$

$$y_B = -c \frac{b_1(X_i - X_0) + b_2(Y_i - Y_0) + b_3(Z_i - Z_0)}{c_1(X_i - X_0) + c_2(Y_i - Y_0) + c_3(Z_i - Z_0)}$$

$X_0, Y_0, Z_0$  describe the position of the projection center,  $c$  is the calibrated focal length. The coefficients  $a_i, b_i, c_i$  are elements of the rotation matrix.

If image coordinates  $x_b, y_b$  and elevation  $Z_i$  of a sample point are known, it is possible to determine its ground coordinates  $X_i, Y_i$  using Eq. 3, which can be derived from Eq. 2.

$$X_i = \frac{((a_2c_3 - a_3c_2)y_B + (b_3c_2 - b_2c_3)x_B)/c + a_2b_3 - a_3b_2}{((a_1c_2 - a_2c_1)y_B + (b_2c_1 - b_1c_2)x_B)/c + a_1b_2 - a_2b_1} (Z_i - Z_0) + X_0 \quad (3)$$

$$Y_i = \frac{((a_1c_3 - a_3c_1)y_B + (b_3c_1 - b_1c_3)x_B)/c - a_3b_1 + a_1b_3}{((a_1c_2 - a_2c_1)y_B + (b_2c_1 - b_1c_2)x_B)/c + a_1b_2 - a_2b_1} (Z_0 - Z_i) + Y_0$$

For each position in the photograph, its location in ground coordinates can be approximated by projective transformation (Eq. 1). Based on these coordinates, the elevation can be interpolated in a digital terrain model. With this elevation information, we can use Eq. 3 to obtain a better approximation of the ground coordinates. This process is repeated until the differences between two iterations are sufficiently small.

### 3.3 Interpolation in a distorted grid

In contrary to WALDHÄUSL,ENTHOFER,KAGER(1986), who search the point of intersection of the optical ray with the DTM, we choose an indirect method. In a first step,all grid points of the DTM are jected in the image plane, according to the parameters of absolute orientation received by intersection in space. Therefore we receive two grids in image coordinates (Fig. 2)i.e. a regular one, representing the sample points, and a distorted one, showing the location of the DTM grid in image coordinates. With the aid of these, we are now able to interpolate ground coordinates of sample points between neighbouring DTM points. For interpolation, different methods become feasible. A plane affine transformation yields best results.

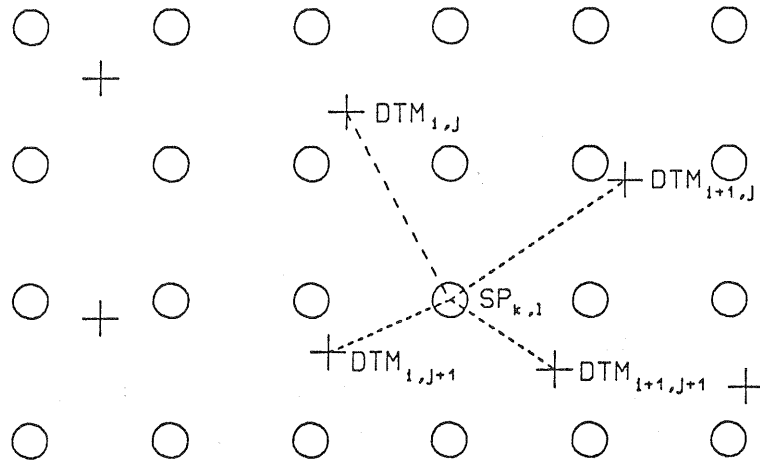


Figure 2: Interpolation in a distorted grid. DTM points are represented by crosses, sample points by circles. Ground coordinates of sample point  $SP_{k,l}$  can be calculated by interpolation between its four next DTM points.

### 3.4 Procedure

After interpretation the data of each interpretation film (tree species, damage class) are entered manually in a data file (matrix file) according to their location in the sample grid. Each sample is related with coordinates in this data matrix.

From the CIR photograph and corresponding maps location and height of at least five control points per interpretation film are determined, marked on the film, and registered in a control point file.

Rectification is performed with the aid of a digitizing table. After having fixed the CIR photograph onto the digitizing table, the interpretation film is fitted to the fiducial marks. By digitizing the fiducial marks the inner orientation is established. Absolute orientation can be obtained by spatial resection using image and ground coordinates of control points.

Up to this point, image coordinates can be transformed into ground coordinates using a DTM, but it is not yet possible to convert the samples stored in the raster data file to image coordinates. Therefore we have to set up a relation between these two systems: The image coordinates of four sample points and their corresponding location in the data matrix determine the coefficients of a plane transformation of now all matrix elements to image coordinates.

Now all for rectification necessitated parameters are available. For each sample in the raster data file, image coordinates can be calculated and its ground coordinates are determined by one of the above mentioned rectification methods.

### 3.5 Restitution Quality

For accuracy determination, the image coordinates of control points were integrated in the rectification process. The residuals obtained by comparing transformed coordinates with coordinates digitized from maps are an estimation for the restitution accuracy (Table 1). The accuracy fits half the resolution of raster elements used for data combination and evaluation in the raster based GIS.

Procedure	Planimetric RMSE (m)	Altimetric RMSE (m)
Projective transformation	20.6	—
Image coordinates and terrain height	10.5	5.0
Interpolation in a distorted grid	9.1	4.9

Table 1: Restitution Quality

## 4 Cartographic Representation

For both study areas, a forest damage map (scale 1:10000 resp. 1:20000) has been created. The location of each sample tree is signed by a cross. The colour represents the corresponding damage class (Fig. 3). The maps allow a good synopsis on the spatial distribution of the damage sites. To enable better interpretation additional geographic features like roads, settlements etc. are added.

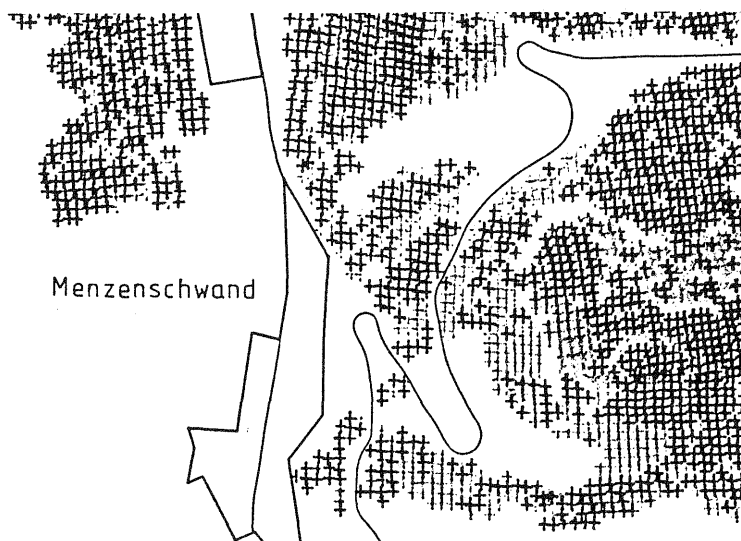


Figure 3: Part of the forest disease map. Dark colours represent high damages, light colours low damages.

## 5 GIS Methodology

Because of the great amount of point data, evaluation was performed on a grid based GIS. The software consists of several procedures and modules which were developed according to the specific needs during this project. The grid based evaluation provides several benefits for such studies:

Area	Tree Species	Damage Class				Number
		0	1	2	3	
Schluchsee	all	35.7	31.0	24.9	8.4	36542
	spruce	34.4	30.3	26.2	9.1	29191
	fir	13.8	29.8	40.7	15.6	456
	beech	45.2	42.5	11.9	0.3	1800
Kälbelescheuer	all	31.8	31.3	28.8	8.2	9136
	spruce	29.8	25.0	32.0	13.2	3493
	fir	19.6	31.5	39.2	9.7	2434
	beech	41.3	39.4	18.4	0.9	2506

Table 2: Damage distribution (%)

- Easy implementation of algorithms,
- high performance for overlay operations,
- high performance for proximity analysis.

An interface to the digital image processing system DIDAK (WIESEL, 1985) allows the use of its processing capabilities, and supports the creation of raster based thematic maps.

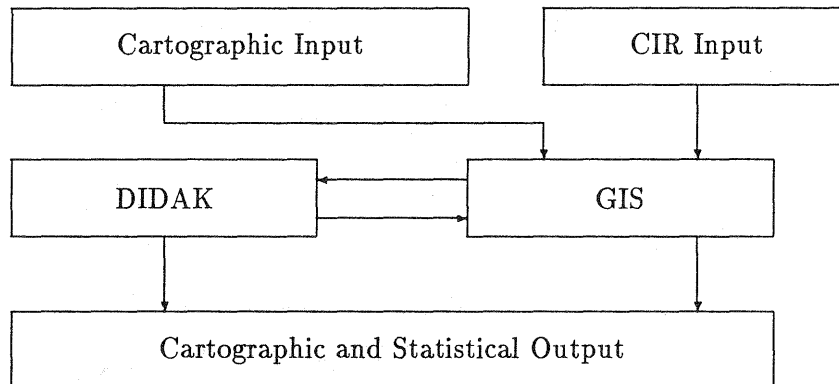


Figure 4: Software Modules

Additional cartographic input can be digitized in vector format. For combination with the forest damage data a vector/raster conversion is performed in the GIS.

## 6 Combined evaluation of forest damage data and ancillary data

### 6.1 Overall result

In Table 2 the distribution of damage classes in both study areas is referred. The amount of samples allows stratification for tree species fir, spruce, and beech. Table 2 can be used for comparison with other results. It turns out that fir has highest damage rates in both areas. Deciduous trees as beech are significantly less damaged than coniferous trees.

Compared with other forest damage inventories (HILDEBRANDT et al. 1987, ZIRM et al. 1985) the damages are considerably higher.

Elevation [m]	Damage Class			
	0	1	2	3
600 - 650	45.7	35.5	13.2	2.6
- 700	50.6	31.8	13.8	1.7
- 750	40.5	38.8	18.0	2.7
- 800	33.9	43.0	20.4	2.7
- 850	35.7	37.5	21.9	3.9
- 900	23.6	38.1	31.6	6.7
- 950	20.8	33.3	37.8	8.0
- 1000	33.5	27.9	29.9	8.4
- 1050	35.4	30.8	26.2	7.6
- 1100	32.7	25.7	29.1	12.4
- 1150	26.3	23.9	36.4	13.4
- 1200	16.7	32.2	38.9	12.2

Table 3: Damage distribution (%), stratified for elevation

## 6.2 Forest Damage Data and Terrain Features

For the Kälbelescheuer area the results (Table 3) show an increasing damage up to an elevation of 900 – 950 m, followed by a zone of reduced damages (up to 1050 m) and again of increasing damages.

Stratifying for single tree species the results are varying. The above mentioned trend is proved true for spruce whereas fir varies from one elevation zone to the next. For the Schluchsee area, the results are quite similar.

The most important result is the existence of a critical elevation level (950 – 1000 m), which has a damage maximum to show. This fact can be interpreted as caused by the upper border of an inversion layer with increasing  $NO_x$  content where  $O_3$  and PAN are created by influence of UV irradiation (SCHÖPFER/HRADETZKY, 1984). High damages above 1100 m can be caused by Ca - and Mg - deficiency (REHFUESS, 1988).

Further evaluation shows that damage increases slightly with increasing slope. However, this effect is mixed with the influence of terrain height.

For examination of exposition caused effects, damages were stratified according to different azimuths. For the Schluchsee area, damages occur increasingly in south west exposed stands while north west exposed trees are less damaged. At the Kälbelescheuer area, a damage maximum can also be found at south west exposed slopes. In this area however, north west exposed stands are also strongly damaged.

Furthermore, we tried to find out hilltops and hollows based on DTM evaluation. By overlaying hilltops and hollows with damage data, trees on hilltops showed tendency to stronger, trees on hollows tendency to smaller damage rate.

## 6.3 Combined Evaluation of Damage Data and Stand Conditions

Typical stand characteristics like age, crown closure, species composition, and stand densities have been estimated during forest inventory. For each stand, these data have been digitized and, after vector/raster conversion, stored up in a data layer for further combined evaluation. Age is the predominating factor for damages (Table 4), especially for coniferous trees. Old trees can have four times stronger damages than young trees.

Stands with high crown closure are significantly less damaged than stands with low density.

Age Level	Damage Class				Number	Percentage
	0	1	2	3		
1	46.0	30.6	18.2	5.2	363	4.1
2	53.2	32.3	12.7	1.8	886	10.0
3	50.5	33.6	13.4	2.5	1657	18.7
4	39.8	32.2	20.7	7.3	1237	13.9
5	19.1	30.7	39.3	10.9	3374	38.0
6	16.0	29.3	41.2	13.5	1361	15.3

Table 4: Damage distribution, stratified for different ages (Kälbelescheuer)

Object	Distance (m)	Damage class				Number
		0	1	2	3	
Roads	25	35.3	32.7	24.9	7.1	481
Main Roads	25	26.9	38.2	26.9	8.0	637
Railway	50	34.7	32.9	26.9	5.5	577
Settlements	125	13.5	32.8	38.6	15.1	119
	250	28.9	28.6	32.4	10.1	706
	500	37.7	29.9	24.8	7.6	3011
Stream courses	25	36.8	33.1	26.1	4.0	329
	50	34.8	33.6	26.8	4.8	560

Table 5: Proximity analysis

Species composition however is of less importance.

#### 6.4 Proximity Analysis

Corridors along roads, rivers, lakes, railroads, and settlements were generated and overlaid with damage data. The results can be reviewed as follows (Table 5):

- Along small roads, damage is smaller than along main roads.
- In the surroundings of the railway which runs in a distance of 100 – 400 meters parallel to one of the main roads, damages are significantly less despite older stands.
- In the environs of settlements, damages are increased significantly.
- In the environs of lakes and rivers, damage values are reduced.

## 7 Conclusions

Based on above mentioned results, statistical evaluation of trees with damage increasing attributes has been performed. The results verify significantly, how the damage distribution is influenced by age, slope, and crown closure (Table 6). At the current state of this study, the results of SCHÖPFER/HRADETZKY (1984) could be confirmed largely. Regarding the main damage increasing factors height, exposition, slope, roads, and settlements, a mayor influence of aerial pollutant on damage distribution can be assumed.



Age level	Crown closure	Slope (gon)	Damage class (%)			
			0	1	2	3
all	closed	0 - 100	34.4	30.3	26.2	9.1
all	closed	> 25	28.8	31.8	27.5	11.9
5 - 6	no closure	> 25	7.4	26.3	43.2	23.0

Table 6: Combination of damage increasing factors

## 8 Acknowledgements

The authors wish to thank the *Forstliche Forschungs- und Versuchsanstalt Baden-Württemberg* for the forest inventory, the *Landesvermessungsamt Baden-Württemberg* for providing the DTM. This project has been funded by the *Project Europäisches Forschungszentrum für Maßnahmen zur Luftreinhaltung* at the Nuclear Research Center, Karlsruhe.

## 9 Literature

- HILDEBRANDT, G. (1984): Zur Festlegung und Lagedefinition der Stichprobenorte im Luftbild bei der Waldschadensinventur Baden-Württemberg 1983 und möglicher Folgeinventuren. - Mitt. d. Forstl. Versuchs- und Forschungsanstalt Baden-Württemberg, Heft 111, S. 119 - 130, Freiburg 1984
- HILDEBRANDT, G., GRUNDMANN, O., SCHMIDTKE, H., TEPASSÉ, P.: Entwicklung und Durchführung einer Pilotinventur für eine permanente europäische Waldschadensinventur. - KfK-PEF 12 (1987), Band 1, S. 45 - 59, Karlsruhe 1987
- KÖLBL, O., TRACHSLER, H. (1980): Regional land use survey based on point sampling on aerial photographs. - ISPRS Congress, Vol. XXIII B 10, S. 536 - 549, Hamburg 1980
- REHFUESS, K.E.: Übersicht über die bodenkundliche Forschung im Zusammenhang mit den neuartigen Waldschäden, Proc. KfK-PEF Statuskolloquium, Karlsruhe, 1988
- SCHÖPFER, W., HRADETZKY, J. (1984) : Der Indizienbeweis: Luftverschmutzung maßgebliche Ursache der Walderkrankung. - Forstwiss. Centralblatt 103 (1984)
- WIESEL, J.: Hardware- und Softwareaspekte, in: BÄHR, H.-P.: Digitale Bildverarbeitung, H. Wichmann Verlag, Karlsruhe, 1985
- ZIRM, K. et al. (1985): Erhebung der Vitalität des Waldes in Vorarlberg. Österreichisches Bundesinstitut für Gesundheitswesen, Wien 1985